Journal of Neuro-Oncology **53:** 243–257, 2001.

Laboratory Investigation

Magnetic resonance imaging of ethyl-nitrosourea-induced rat gliomas: a model for experimental therapeutics of low-grade gliomas

Phillip E. Kish[1], Mila Blaivas[2], Myla Strawderman[3], Karin M. Muraszko[1], Donald A. Ross[1], Brian D. Ross[4] and Gerald McMahon[5]
[1]*Department of Neurosurgery,* [2]*Department of Pathology,* [3]*The Comprehensive Cancer Center,* [4]*Department of Radiology, University of Michigan Medical School, Ann Arbor, MI;* [5]*Sugen Incorporated, South San Francisco, CA, USA*

Key words: magnetic resonance imaging, ENU, transplacental induction, N-ethyl-N-nitrosourea, gliomas

Summary

Human low-grade gliomas represent a population of brain tumors that remain a therapeutic challenge. Preclinical evaluation of agents, to test their preventive or therapeutic efficacy in these tumors, requires the use of animal models. Spontaneous gliomas develop in models of chemically induced carcinogenesis, such as in the transplacental N-ethyl-N-nitrosourea (ENU) rat model. However, without the ability to detect initial tumor formation, multiplicity or to measure growth rates, it is difficult to test compounds for their interventional or preventional capabilities. In this study Fisher-334 rats, treated transplacentally with ENU, underwent magnetic resonance imaging (MRI) examination in order to evaluate this approach for detection of tumor formation and growth. ENU-induced intracranial cerebral tumors were first observable in T2-weighted images beginning at 4 months of age and grew with a mean doubling time of 0.487 ± 0.112 months. These tumors were found histologically to be predominately mixed gliomas. Two therapeutic interventions were evaluated using MRI, vitamin A (all-trans retinol palmitate, RP), as a chemopreventative agent and the anti-angiogenic drug SU-5416. RP was found to significantly delay the time to first tumor observation by one month ($P = 0.05$). No differences in rates of tumor formation or growth rates were observed between control and RP-treated groups. MRI studies of rats treated with SU-5416 resulted in reduction in tumor growth rates compared to matched controls. These results show that MRI can be used to provide novel information relating to the therapeutic efficacy of agents against the ENU-induced tumor model.

Introduction

Gliomas comprise the majority of the primary brain tumors diagnosed annually in the United States [1,2]. Of these tumors, low-grade gliomas are relatively common, with low-grade astrocytic tumors alone comprising as much as 15–32% of surgically treated brain tumor [3,4]. These tumors are characterized as having a benign histologic picture, indolent growth, and prolonged survival, but their biologic behavior is unpredictable [5–8]. Some lesions appear curable, but low-grade tumors have been shown to have a propensity to develop anaplastic features [5,7,9,10]. This progression is thought to be due to the genetic instability of the low-grade gliomas, which allows additional genetic deletions, amplifications, and mutational events to occur [11]. This progression or change in tumor grade, can take the life of the patient sometimes decades after initial diagnosis [6,12].

Currently, therapies for low-grade gliomas include observation, resection, radiation, and chemotherapy. Due to the infiltrative nature of gliomas, surgery is rarely curative. In some locations, radical surgery with newer image-guided techniques and functional mapping offers the prospect of prolonged survival by allowing better and more complete surgical excisions. There is controversy about the role of radiation therapy in the management of low-grade gliomas. Some centers have reported no benefit in length or quality of life, while others have detected a small benefit to radiation [13–15].

Chemotherapy regimens, found to have benefit in high-grade gliomas, are currently in trial for low-grade gliomas. Although there is increasing evidence that combination-agent chemotherapy such as carboplatin and vincristine can delay progression of low grade gliomas, long-term outcome data (10–20 year) are not available [16].

The current lack of curative therapeutic options for treatment of low-grade gliomas indicates that alternative therapies need to be considered. However, the scarcity of suitably characterized low-grade glioma models for preclinical testing makes the development of new therapies more difficult. Unfortunately, human low-grade gliomas have not been established in culture, nor is there an *in vitro* model of progression from low-grade to high-grade glioma. Thus, testing of preventative or interventional therapies targeting glial tumor progression currently requires the additional development of *in vivo* animal models.

One potential model for low-grade gliomas is the induction of rat brain tumors with chemical carcinogens. These are reproducible models that have been utilized for over 30 years. However, wide variations in tumor type, location, size, and growth kinetics exemplify the complexity of these brain tumor models. Their main strength however, has been the spontaneous nature of the induced tumors exhibiting the characteristics of progression over time from small early neoplastic proliferations, evolving into large malignant neoplasms. The offspring of rats given a single intravenous dose of N-ethyl-N-nitrosourea (ENU) later than the 13th day of gestation or during early postnatal development, develop malignant neuroectodermal tumors of the central and peripheral nervous systems [17,18]. This tumor incidence approaches 100% in many rat strains [19,20]. The carcinogenic effect is presumably due to the alkylation of DNA by ENU, which occurs rapidly due to the short half-life of the compound. Once completed, the neoplastic transformation remains indolent until a much later time. In this model, early neoplastic proliferation is followed by microtumors and finally visible tumors develop with increasing signs of progression to higher grades of malignancy as indicated by increased mitoses, vascularization, and necrosis. The brain tumors induced by this carcinogen are reported to be primarily astrocytomas, oligodendrogliomas, mixed gliomas, ependymomas, and/or medulloblastomas [21–25]. However, this may be somewhat dependent on the strain of rat. Several recent reports have analyzed the pathology of transplacentally ENU-induced tumors. Zook et al., found that mixed gliomas grew larger, had a shorter latency, and were significantly more malignant than were other gliomas [26]. Mandeville et al., [27] found that 5 mg/kg of ENU was able to induce from 30–46% glial tumors in Fisher-344 rat offspring. Glial tumors (mixed gliomas and oligodendrogliomas) were the most frequent type of tumors observed. Mixed glial tumors were usually quite large and characterized by a mixture of oligodendroglial cells and astrocytes.

There are a limited number of reports testing agents for their preventive or therapeutic efficacy utilizing chemically induced models of CNS carcinogenesis. These studies have usually been designed as survival studies either with or without interim sacrifices to examine tumor incidence. Alexandrov's group in Russia has used the ENU transplacental carcinogenesis model to examine the preventative or interventional effects of a variety of compounds [28–31]. They have examined the vitamins; retinol acetate, alpha-tocopherol acetate and thiamine chloride; the antioxidant sodium selenite; and an inhibitor of polyamine biosynthesis, alpha-difluoromethylornithine (DMFO). DMFO exerted a slight inhibitory effect on tumor incidence, decreased the total CNS tumor multiplicity and the multiplicity of peripheral nervous system tumors. It also prolonged survival time. Retinol, tocopherol, thiamine, and selenite did not influence the development of transplacentally induced tumors [28]. However, all these studies have been hampered by the inability to detect initial tumor formation, multiplicity, and growth of the resulting tumors, in addition to survival of individual animals. The large variation in the time to occurrence and location of the resulting occult tumors has been a tremendous limitation of this model.

Non-invasive MR imaging has demonstrated the capability to perform repeated measurement of tumors derived from orthotopically implanted cell lines and to measure changes in growth rates caused by therapy [32]. Additionally, ENU-induced tumors have been reported as imagable by magnetic resonanace imaging (MRI) [33–36]. To date, no study has reported the effect of any therapy on chemically induced brain tumors true incidence or growth rates. We, therefore, investigated the capability of repeated MRI measurements to obtain a more accurate determination of the incidence, number and growth rate of tumors in ENU-treated animals. We chose to test two different therapies based upon their different modes of action. We had previously found vitamin A to increase survival in ENU-treated animals

fed a diet with increased vitamin A [37]. Statistical analysis suggested that the mechanism of action was a delay in time to tumor formation, a chemopreventative action. Tumor growth is also dependent upon blood supply. Vascular endothelial growth factor (VEGF), by inducing angiogenesis, has been implicated as a major paracrine mediator of glioma development by stimulation of angiogenesis [38–40]. Inhibition of VEGF receptor 2 (FLK-1/KDR) tyrosine kinase activity has been shown to effectively block angiogenesis and tumor growth of gliomas implanted in rat dorsal skin chambers [41]. We, therefore, examined the effect of SU-5416, a small molecule inhibitor of the VEGF receptor FLK-1, as an interventional therapy to block the growth of small ENU-induced tumors.

Materials and methods

Chemical induction of brain tumors

As in our previous experiment, tumors were induced by transplacental exposure [37]. Timed-pregnant Fisher-334 dams were injected via the lateral tail vein on the 21st day of gestation with 50 mg/kg of a 0.1 M solution of ENU (Sigma, St Louis, MO) dissolved in citric acid: disodium phosphate buffer (pH 6.0) immediately prior to injection. Due to the limited diameter of the head coil used in the MRI scanner, we wanted to ensure that the animal's head could be imaged at one year of age. The Fisher-344 rat strain was chosen as this strain produces small sized animals known to be susceptible to ENU tumor induction [20,26,27]. Second, the animals were exposed to ENU on day 21 of pregnancy, a time shown to cause the greatest number of brain tumors in their offspring [42]. The offspring were delivered naturally, were whelped by their natural mothers, and weaned at 21 days of age.

Retinol palmitate dietary treatment

All pups (26) from three dams were randomly assigned to control (ENU exposed) or all-trans retinol palmitate (RP) treated ENU-exposed groups (8 females, 5 males; 13 animals/group). All animals were housed in groups based on sex and treatment groups, and had access to food and water *ad libitum*. RP-treated animals received standard chow supplemented with 150,000 IU vitamin A palmitate/kg (Sigma, St Louis, MO) as previously described [37,43]. This was accomplished by stirring standard chow (Purina 5001) in an ethanol solution of RP for 1.5 h in the dark, during which time most of the ethanol evaporates. Although no direct measurement of vitamin A status of the animals was made, our previous experiment had shown that 150,000 IU of dietary vitamin A caused a change in survival in rats. Historically, this concentration has been utilized to study the effect of vitamin A on wound healing in rats, including local tumor irradiation or cyclophosphamide treatment [43]. This concentration is approximately 10 times the basal dietary concentration of vitamin A found in normal rat chow (approximately 15,000 IU vitamin A and 6.4 mg β-carotene/kg) which exceeds the recommended minimum daily allowance for rodents. Animals on both diets gained weight corresponding to the normal growth curves for their strain. ENU-induced dams and ENU-control offspring were fed standard lab rodent chow treated with ethanol alone (ENU control animals). Food was replaced twice a week. It was prepared at one-week intervals and stored at 4 °C.

Animals with no reported death or autopsy, were censored after the last known time of imaging or observation. This censoring affected survival analysis and percentage of animals with a given tumor histology.

Magnetic resonance imaging

Monthly MRI images were obtained beginning at 2 months of age. Animals were imaged every month (months 2–8) for the purpose of determining the incidence, number, and growth rate of each tumor. Animals were anesthetized with 2% isoflurane in air during the imaging sessions. All *in vivo* MRI experiments were performed on a Varian system equipped with a 7.0 Tesla, 18.3-cm horizontal bore magnet (300 MHz proton frequency). Each MRI session acquired T2-weighted images through the rat brain, which were produced using the following parameters: TR/TE = 3,500/60, FOV = 30 × 30 mm using a 256 × 128 matrix; slice thickness = 0.5 mm; number of slices = 50; slice separation = 0.0 mm by interleaving two sets of 25 slices. The 0.5-mm interleaved sections routinely allowed detection of tumors as small as 1 mm in diameter. We limited this experiment to the imaging of intracranial cerebral tumors. This eliminated leptominengeal tumors, schwannomas, and several other tumor types. The most relevant tumor diagnosis for the remaining tumors was

oligodendrogliomas, astrocytomas, mixed gliomas, or ependymomas. Tumor volume determination of the first tumor formed from serial image slices was accomplished as described [32]. Tumor volumes measured excluded any cyst volume present.

Histologic evaluation

Brains and spinal cords were dissected free from the cranium or spine and fixed by immersion fixation in 10% buffered formalin. Spinal cord tumors were visually determined with the aid of a dissecting microscope. To evaluate the histopathology of each MRI lesion, a 5-μm thick paraffin-embedded section of the brain corresponding to the MRI imaged lesion was stained with hematoxylin and eosin. All paraffin sections were examined by a neuropathologist (MB) blinded as to the group and age of the lesion. Each neoplasm was diagnosed and graded according to the criteria described by Zook et al. [26]. In the case of heterogeneous tumors, tumors were graded at the highest grade observed.

Additionally, paraffin sections of the cerebral tumors used in the measurement of tumor volume (first intraparenchymal tumor formed in the cerebrum of the rat) were immunostained with anti-vimentin and anti-glial fibrillary acidic protein (GFAP) antibodies according to supplier recommendations. The immunohistological examinations assisted the diagnosis of oligodendroglioma, astrocytoma, or mixed gliomas in the tumors.

Anti-angiogenic therapy

To test the effect of the VEGF receptor inhibitor SU-5416 (Sugen, San Francisco, CA), tumors were induced in rats as described above, which were initially imaged by T2-weighted MRI when the animals were 5 months of age. Animals with tumors with smaller than 0.35-mm diameter were randomly divided into control and treatment groups. Treated animals received 50 mg/kg of SU-5416 twice a week in a controlled release formulation. Control animals received the suspension diluent alone. Animals were generally imaged twice a week utilizing T2 weighting with either 0.5 or 1 mm thick slices with a TR/TE = 3,000/60. Tumor volumes were measured as described above. T1-weighted images with and without gadolinium contrast agent were acquired in selected animals during treatment with the SU-5614 compound as detailed in the figure legends.

Results

Development of ENU-induced tumors

Intracranial tumors induced by transplacental induction with ENU first became visible by MRI beginning at 4 months of age in the control animals. ENU-induced tumors appeared as a black T2-hypointense mass, frequently associated with a T2-hyperintense ring (white) surrounding the mass (Figure 1). After a period of tumor growth (generally one or two months), alterations in the signal intensity of the T2 images were observable within many of the tumors (Figure 2, Month 2). These alterations had the appearance of a reticular network in the MRI's, which appear to correlate with the appearance of endothelial proliferation observed in histological sections of these tumors (Figure 3). Additional data shows these reticular areas as developing vascular elements of the tumors. T1-weighted imaging with gadolinium contrast enhancement (Figures 4a,b) shows contrast enhancement of these areas, but not of the more hypointense areas, which are presumably tumor cells. Later still was the appearance of cysts within the tumor (Figure 2, Month 3). Cyst development is consistent with an increase in vascular permeability, as evidenced by increased gadolinium contrast enhancement with T1 imaging (Figure 4a). All tumors with cysts were found to be high-grade tumors, suggesting that cyst formation is a marker of progression of tumors in this model. These tumor masses could continue to increase in size for several months before any neurological deficits were observed.

Effect of dietary retinol on measurement of time to first tumor and tumor multiplicity

Dietary RP produced a significant delay in the time to first tumor (TTT) compared to ENU controls. Figure 5

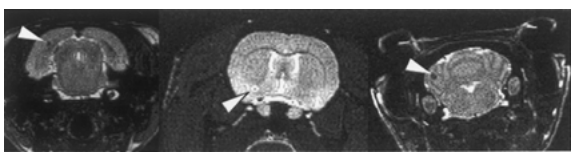

Figure 1. Detection of ENU-induced brain tumors. Transplacental ENU-induced tumors (50 mg/kg on day 21 of pregnancy) were detected by imaging with T2-weighted MRI. Representative images of several different small early tumors, showing a low signal intensity core mass with a hyper-intense peripheral ring.

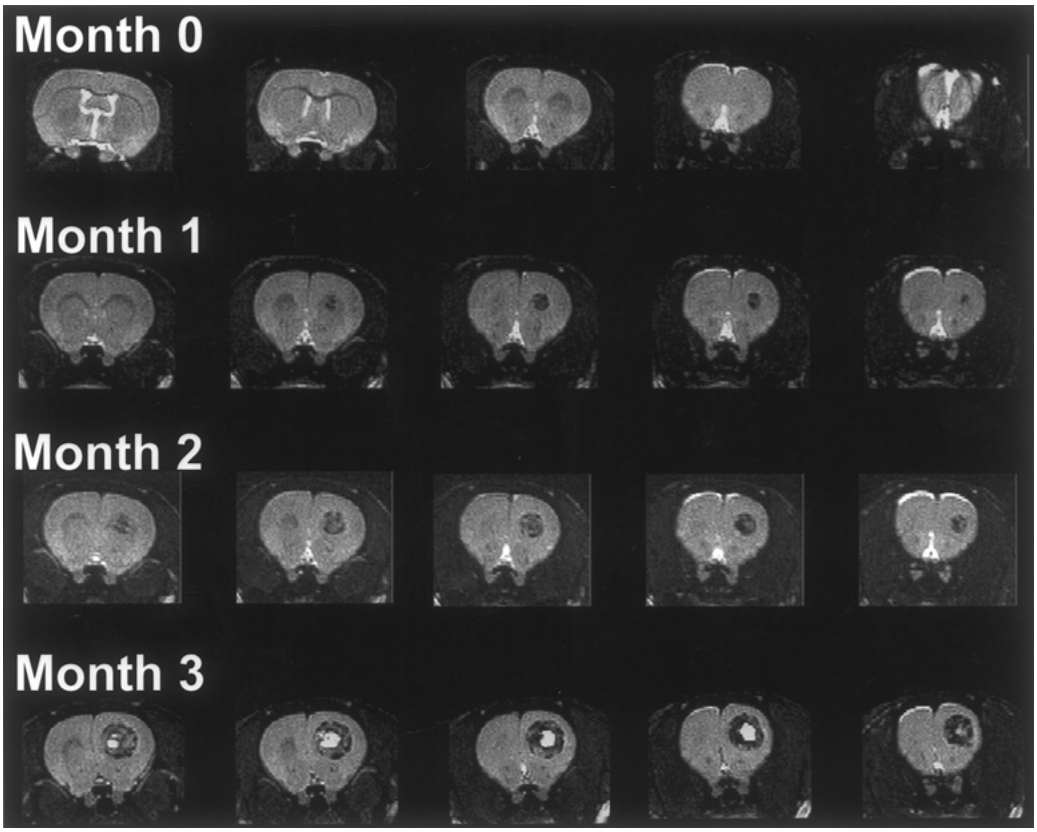

Figure 2. Growth of ENU-induced brain tumors. MRI images of a representative tumor over several months. Tumor masses exhibited slow growth, characterized by slow expansion of the low signal intensity core. In addition, a number of tumors developed cysts after several months of growth.

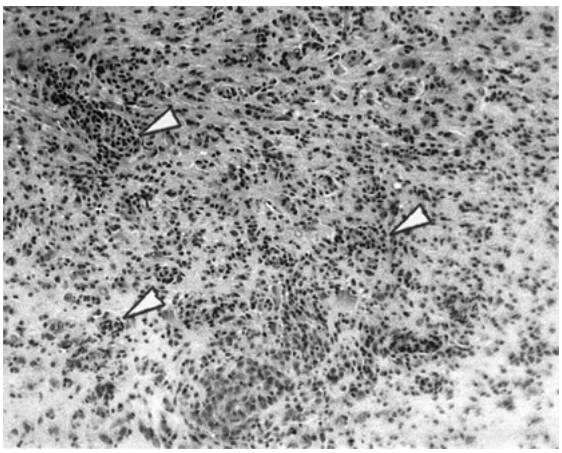

Figure 3. Histology of a tumor with reticular network appearance on the MRI. H&E stain of tumor shows extensive proliferation of the vascular endothelium, indicated by white arrows.

shows that rats ingesting 150,000 IU/kg of feed of RP exhibited a shift in the TTT curve of approximately 1 month (Wilcoxon log rank test, $P = 0.05$). The effect of RP on delaying tumor formation is transitory, with the largest effect being observed during months 4 and 5. After this time greater than 75% of the animals in both groups had developed their first tumor.

Taking advantage of the repeated measures within each animal, the total number of tumors at each imaging session was determined by counting tumors in each contiguous serial slice. Figure 6a shows the average number of tumors in surviving animals each month. Commonly, tumor multiplicity is determined at a single time point at animal sacrifice when the total number of tumors is counted. Since imaging allows determination of tumor multiplicity without animal sacrifice, we were able to determine tumor multiplicity monthly for each animal. We also determined the rate of new tumor formation from the time of first tumor occurrence.

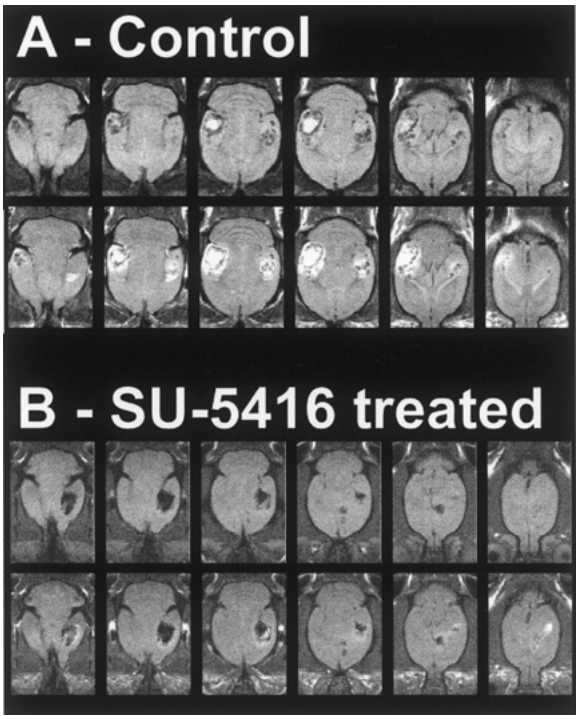

Figure 4. T1-weighted MRI of tumor vasculature and cyst. T1-weighted images were acquired (TR/TE = 750/30) without contrast (upper panels of A & B). 2 ml of 25 mM gadolinium contrast agent (Magnavist) were given via an I.P. catheter and a series of images collected over the next half-hour. Lower panels of A and B were collect 20 min after contrast injection. SU-treated tumor has much lower amounts of contrast enhancement suggesting less vascular permeablity.

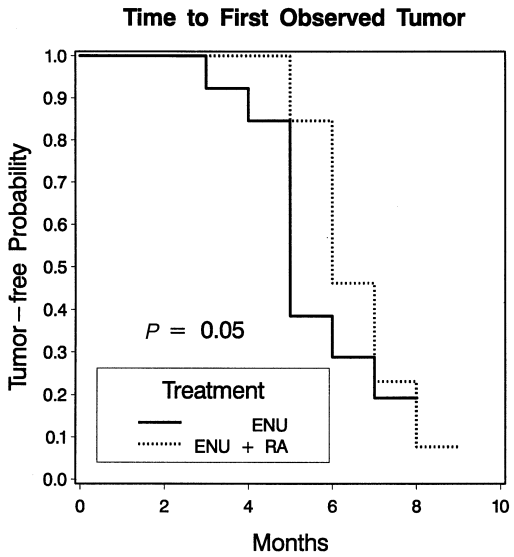

Figure 5. Retinol delays time to first tumor. Dietary retinol palmitate (150,000 IU/kg of chow) significantly delayed the appearance of the initial MR imagable tumor by approximately one month (Wilcoxon log rank test, $P = 0.05$). Tumors were detected on contiguous 0.5-mm thick sections.

Shown in Figure 6b, the rate of formation of the new tumors was analyzed using a generalized linear mixed model. The number of new tumors in each month is assumed to follow a Poisson distribution, based on an analysis of the residuals. A logarithmic link is used to relate the mean of this Poisson to a quadratic function of time for each treatment. The plot in Figure 6b shows the mean estimated rate of tumor formation for each treatment arm as a function of time from formation of the first tumor. The difference in the linear component of the rate of tumor formation between the ENU control group and RP treated animals was not significantly different ($P = 0.89$). There is some suggestion that the non-linear component of the rate of new tumor formation (i.e. the curve of the line) may be different between treatments ($P = 0.04$). However, there is limited data for RP treated animals having tumors for 4 months or longer that may influence the estimation of the curvature. Thus, RP appears to delay the time to occurrence for multiple tumors, but the rate of formation is unchanged.

Effect of dietary retinol palmitate on tumor growth rates

Using repeated MRI measurements, we were able to quantify changes in tumor volumes over time. Figure 7 shows the changes in the first tumor volumes for animals in which the first apparent tumor was within the cerebrum, a location that is generally consistent with mixed glioma histology. Tumor growth rates showed mean doubling times of 0.487 ± 0.112 and 0.559 ± 0.153 months for ENU and ENU+RP treatments, respectively, a non-significant difference.

Tumor histology

A neuropathologist (MB) graded the tumors as low to high grades of malignancy using the criteria described by Zook et al. [26]. In the case of heterogeneous tumors, they were graded at the highest grade observed. Tumor histology of all tumors found at the end of the animal's life showed a mixture of low- to high-grades (Table 1), consistent with previous observations in this brain tumor model. There appeared to be

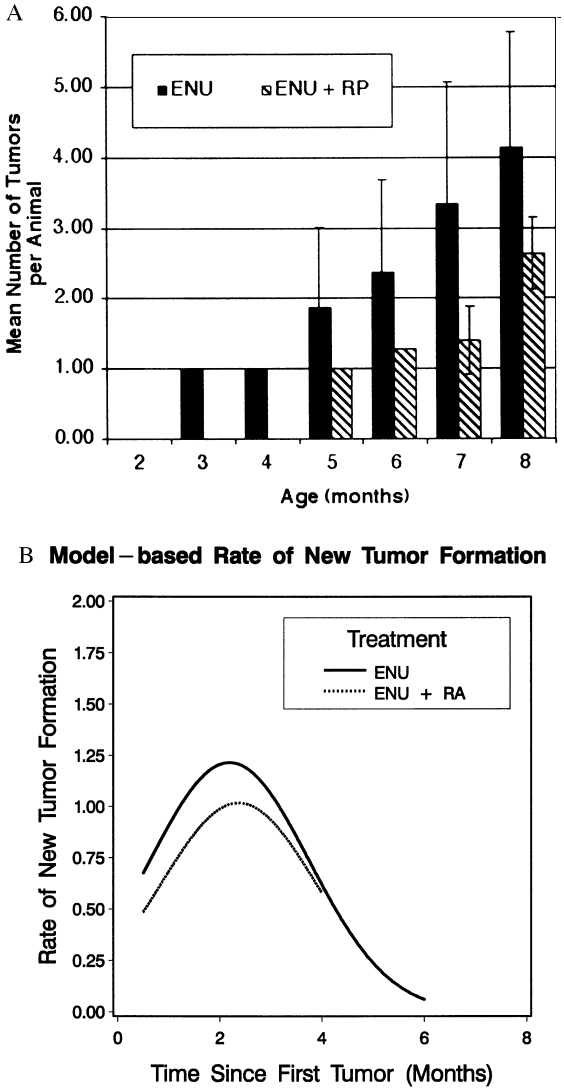

Figure 6. Detection of tumor multiplicity. The number of tumors in each animal brain was determined at each imaging session. Panel (A). The mean number of tumors per tumor bearing animal ± SD. Panel (B). The rate of formation of the new tumors analyzed using a generalized linear mixed model. The number of new tumors in each month is assumed to follow a Poisson distribution. A logarithmic link is used to relate the mean of this Poisson to a quadratic function of time for each treatment. The plot shows the mean estimated rate for each treatment arm as a function of time from formation of the first tumor for each animal. No significant difference was detected.

a large dichotomy in the tumor grading. Tumors that had progressed beyond the low-grade criteria had variable regions of high-grade morphology, thus there were no 'pure' intermediate grade tumors. Several of the

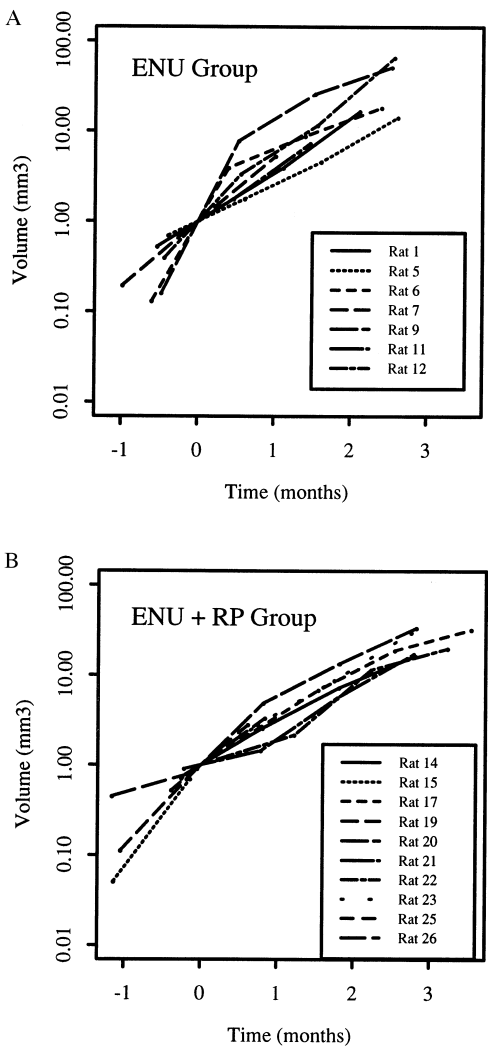

Figure 7. Measurement of tumor growth rates. Tumor volumes were quantified for animals in which the first tumor was found intracortically. Growth rates were determined for both control (A) and RP-treated (B) animals. The plots show the changes in tumor volume over time, with the curves shifted to adjust the intercepts of the curves to be normalized to 1 mm^3.

Table 1. ENU histopathological tumor grading

	Low grade	High grade	Total
ENU control	9	26	35
Retinol palmitate	10	28	38

Tumors were identified and graded in paraffin sections obtained from blocks containing the MRI identified tumors. Microscopic as well as macroscopic tumors are included in the table. No differences were found in either the number or ratios of tumor grades.

low-grade tumors were microtumors, which were not imaged by MRI.

Of the tumors that were quantified for growth rates described above, with the exception of one low-grade oligodendroglioma, all were high-grade mixed gliomas. These showed increased mitotic figures, approximately 50% with marked nuclear pleomorphism, and approximately 20% with undifferentiated small cell clones. High-grade tumors showed necrosis, marked endothelial proliferation and individual cell necrosis. Many tumors also appeared to have entrapped neurons as a part of the neoplasm. The mixed-gliomas displayed a variable proportion of oligodendrocytes to astrocytes as determined from immuno-histochemistry (Figure 8).

Effect of dietary RP on survival

Although RP delayed time to first tumor formation (TTT), in this experiment dietary RP did not produce a survival advantage. Figure 9 shows the Kaplan-Meier survival curve for the two groups. Dietary supplementation of RP although suggestive, did not increase survival significantly over the ENU control group ($P = 0.18$, Wilcoxon test). Early increased survival by RP did not extend indefinitely as the survival curves merge towards the end of the experiment at 11–12 months. However, RP-treated animals developed a larger number of spinal cord tumors causing hind leg paralysis, these were confirmed at autopsy (6/12 animals with RP treatment vs. 3/12 animals for controls). The development of spinal cord tumors or other additional secondary tumors with increasing age may have altered the survival analysis.

Effect of anti-angiogenic therapy on tumor growth rates

We treated rats with small ENU induced tumors, in a second experiment, to examine the therapeutic potential for the anti-angiogenic drug SU-5416 in this model. Changes in tumor volumes for control ($n = 3$) and SU-5416 treated animals ($n = 3$) were determined at 4–7 day intervals (Figure 10). Tumor growth in control animals was as described above in the RP experiment, with two of the three animals developing cysts within one of their tumors and subsequently sacrificed due to neurological impairment (Figure 10 upper left panel and Figure 11). Treatment with the drug SU-5416 resulted in reduced growth rates of tumors in two of three treated animals (Figure 10 lower left and right panel and Figure 11) and possibly complete regression of a small tumor in the third (see the discussion section). MR images of the treated tumors showed little change in either size or imaging characteristics such as the development of, or increased amount of the reticular formations suggestive of vascularization. One of the three SU-5416 treated animals developed a tumor cyst suggesting evidence that SU-5416 may not delay the progression of these tumors. Histological analysis supports this observation (Figure 12). For example, in animal 2836 tumor growth was minimal, but the histology of the two tumors in this animal were both classified as high-grade mixed gliomas. These tumors lacked significant vascular proliferation and the remaining vessels were thin walled in contrast to control animals.

Discussion

Past studies, utilizing oncogenetic or chemically induced tumors, have been limited by their inability to determine the precise time and location of CNS tumor occurrence. Alternatively, survival analysis or time to neurological impairment has been used as a parameter in the evaluation of neurooncopreventative agents, but this is a crude endpoint providing little information about tumor incidence or growth. From previous studies, we recognized that testing agents for their preventive or therapeutic efficacy in models of spontaneous carcinogenesis would be difficult without the ability to detect tumor formation or growth, in addition to animal survival. As non-invasive imaging of brain tumors is becoming more common, MRI was used in order to obtain a more accurate determination of the number, incidence, and growth rate of the tumors. Initially applied to transplanted tumor animal models to measure growth, several groups have also used it to detect tumors produced by ENU exposure MRI [33–36].

This study confirmed the progressive growth of ENU-induced brain tumors in this model. It is well documented that ENU induces areas of increased proliferation that form microtumors by 60–90 days of age [44–47]. The growth of these microtumors into macroscopic tumors occurs between 4 and 5 months of age, which correlates with the appearance of the lesion within the cerebrum apparent by T2-weighted MRI. These tumors can frequently be observed as small 0.5 mm (approximately 3-μl volume) although it is difficult to differentiate tumors at this size from

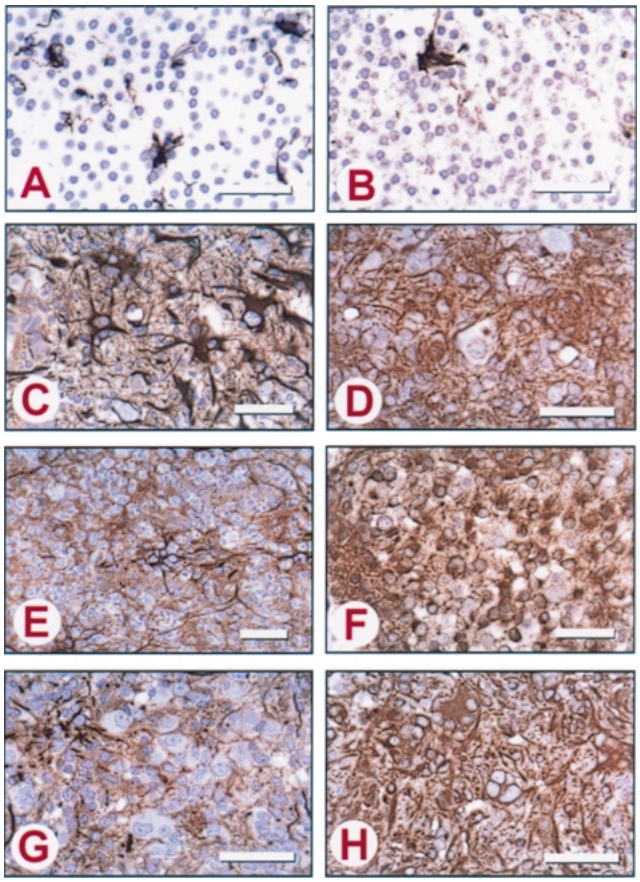

Figure 8. Immunohistochemistry of the ENU-induced tumors for diagnosis of tumor type. Peroxidase reaction with hematoxylin counterstain. Single low grade oligedendroglioma in the entire series. (A) GFAP stained, (B) Vimentin stained. GBM pattern (either as an entire tumor or as a part of a heterogeneous tumor). (C) GFAP stained, (D) Vimentin stained. Tumor composed mostly of glial precursors (E) GFAP stained, (F) Vimentin stained. Nuclear pleomorphism present in the majority of the tumors (G) GFAP stained, (H) Vimentin stained. Bar $= 50\,\mu$m.

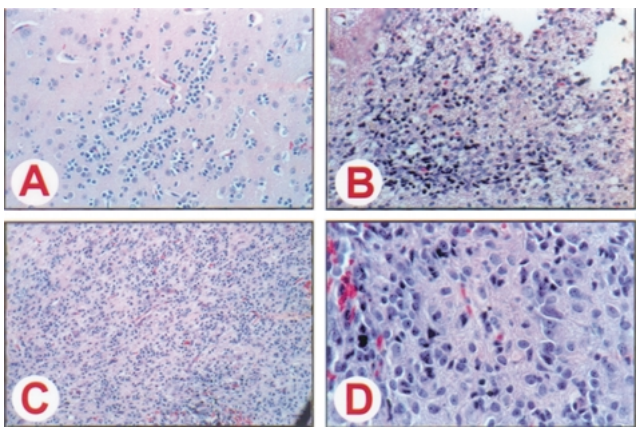

Figure 12. Histology of SU-5416 treated ENU tumors. Panel (A) Gray matter low-grade oligodendroglioma (Figure 11, right panel) margin with neoplastic satellite cells around neurons (164× magnification). (B) Low-intermediate grade oligodendroglioma (230× magnification). (C) High-grade mixed glioma with significantly reduced and thin walled vasculature (115× magnification). (D) Higher magnification of panel C, showing mitotic figures, nuclear pleomorphism, hemaciderin deposits and rare thin-wall blood vessels.

large blood vessels or MRI artifacts. Tumors reaching 1-mm diameter are readily identifiable by T2 weighted MRI. The appearance of a hyper-intense ring on the T2 images at the periphery of the tumor suggests that this may be an area of increased water content, possibly caused by increased vascular permeability. VEGF has been shown to be expressed very early in the brain tumors induced by ENU [48,49]. Increases in vascular permeability are thought to be associated with the angiogenic process and this is further supported by the size of the tumor (~1–2 mm), which is within the range postulated for the development of vascular elements (the angiogenic switch [50–52]). It has been shown that both microvessel density and VEGF levels are independent prognostic markers of survival in fibrillary low- grade astrocytoma in humans [53]. This finding led them to suggest that fibrillary diffuse low-grade astrocytoma is composed of a spectrum of tumors with differing propensities to undergo malignant transformation that is at least partly based on their inherent angiogenic potential. A similar scenario can be envisioned for ENU-induced tumors in this model.

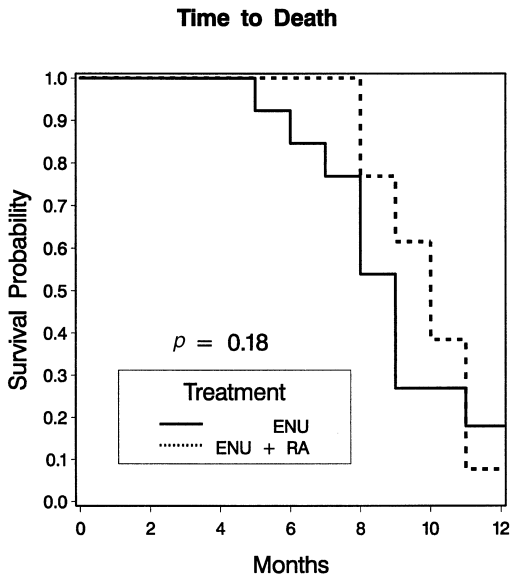

Figure 9. Time to death. The Kaplan-Meier survival curve for the two groups is shown. No significant increase (Wilcoxon log rank test, $P = 0.18$) in survival due to RP treatment was detected.

ENU-induced tumors were found to increase in size throughout the animal's life. Although tumor volume is negatively linked with survival [26], the size of the tumor is not a good predictor of survival, as several animals with extremely large tumors showed no neurological deficits and survived for extended periods (data not shown). Because of the rapid growth rate of the mixed gliomas, we believe that the majority of tumors imaged developed into mixed gliomas, which is supported by the histological and immuno-cytochemical results. The tumor growth analysis for the RP dietary treatment was limited to the first tumor to appear within the cerebrum by MR imaging. We observed that a majority of the macroscopic intracranial tumors induced in the Fisher-344 rat offspring were mixed gliomas thus suggesting a limitation of the potential variation in histological types

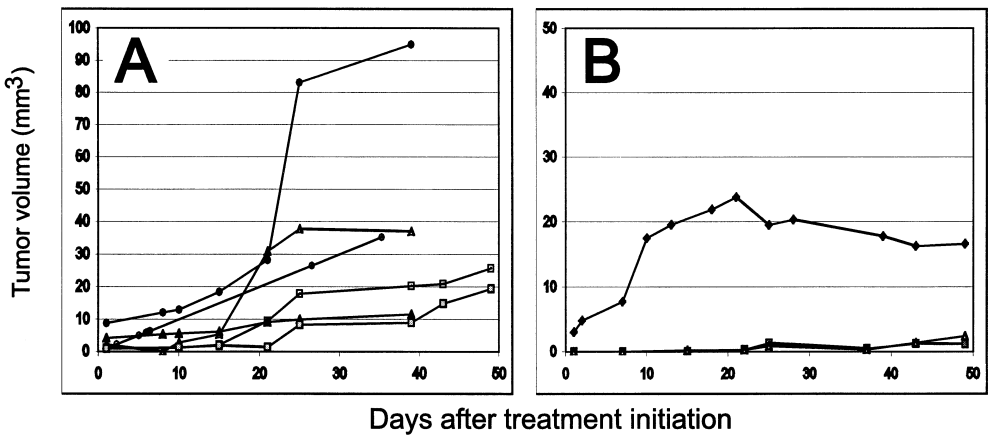

Figure 10. Measurement of tumor growth volumes. Tumor volumes were quantified for animals in which the tumors were found intracortically for both control (A) and SU-5416-treated (B) animals. The plots show the changes in tumor volume over time beginning on the day of treatment. Open and closed symbols indicate multiple tumors in each of the three control animals and one of the SU-5416 treated animals.

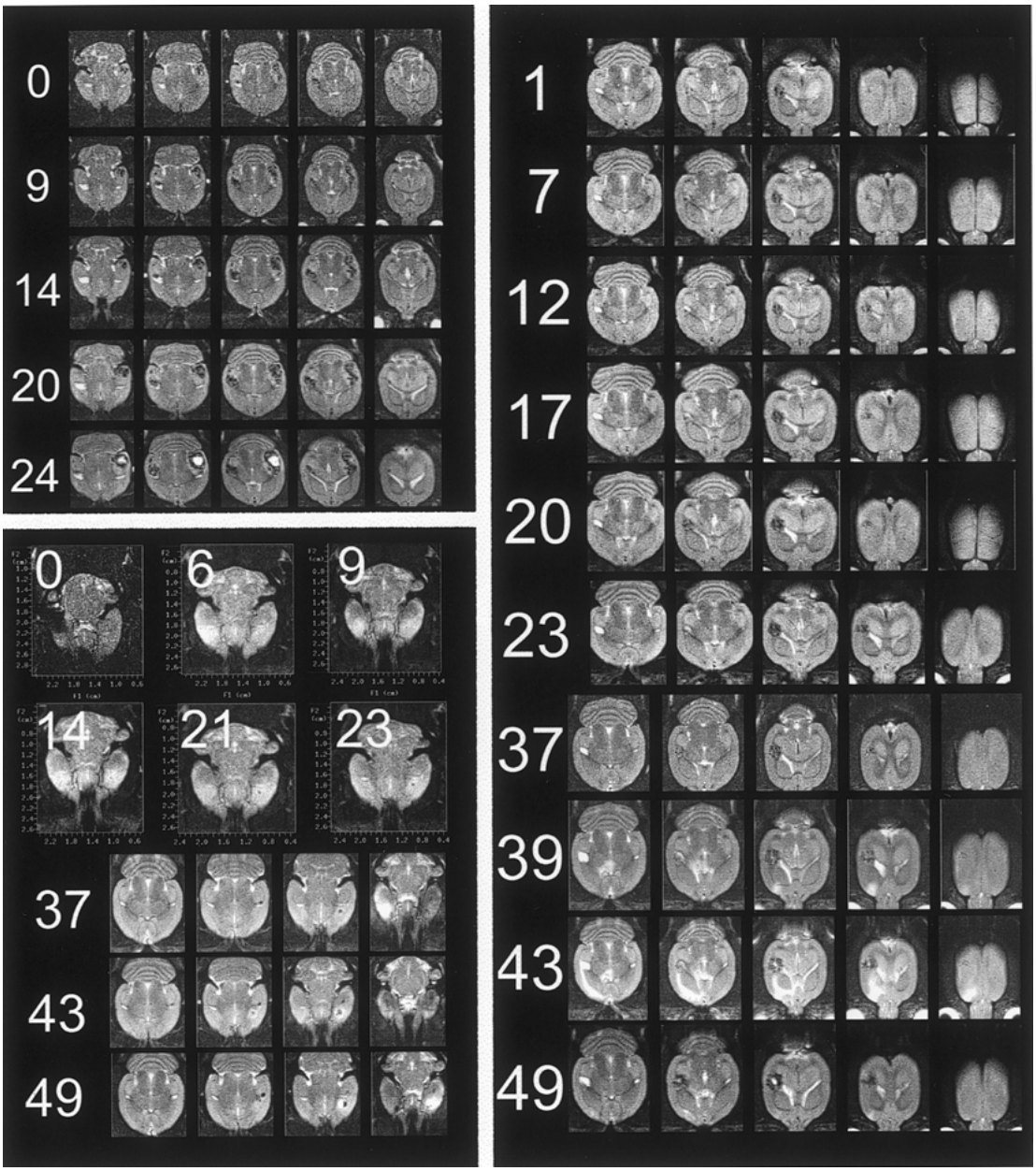

Figure 11. Growth inhibition of ENU-induced brain tumors. MRI images of representative tumors over 49 days. Control animal (upper left panel) had bilateral tumors that exhibited rapid growth with formation of cysts at 24 days of observation. SU-5416 animals in contrast (lower left (high-grade mixed glioma) and right panels (low-grade oligodendroglioma)) exhibited a large reduction in tumor growth rates. SU-5416 animals developed cysts later (49 days) and in smaller tumors than controls.

of tumors induced in this strain. The mean doubling times of 0.487 ± 0.112 months for ENU induced tumors is in general agreement with the 11.03 ± 7.74 days (0.363 ± 0.255 months) observed by Nakajima et al. in Wistar rats [34].

We did not conduct an exhaustive search for early neoplastic proliferations or microtumors. The use of tumor diagnosis at the time of terminal sacrifice describes very little of the 'natural history' of these tumors and is of minimal significance except to reaffirm

the finding that the tumors imaged were generally a homogenous population of mixed gliomas. We believe, based on the literature and our unpublished observations, that there is a strong correlation between the size of a tumor and its grade. Unfortunately, due to the limited number of animals in this pilot study, we were unable to perform interim sacrifices to correlate tumor size with grading. However, all of the large tumors that were imaged and graded as 'high grade' at sacrifice were derived from small tumors. Low-grade tumors were only observed as small tumors. The low number of anecdotal low-grade tumors are reflective of the time of sacrifice (late-stage) and may not be reflective of the tumor histology of the earlier occurring small tumors that progressed to be high-grade, malignant mixed gliomas.

This study, as does our previous one, supports that in the ENU model, retinoids may delay the onset of brain tumor formation, but do not appear to prevent it. This observation is similar to the effect of retinoids in delaying onset of ENU-induced leukemia in mice [54,55]. Our observation that RP increases the latency period for macroscopic tumors is in conflict with an earlier report by Grubbs et al. [56], where retinyl acetate, 13-cis-retinoic acid and all-trans-retinoic acid did not alter the incidence, number or latency period of the induced tumors. However, dosage and chemical form of the retinoid, strain of rat used and methodology used to detect initial tumor formation varied between the two experiments and may explain the discrepancy.

The lack of treatments with therapeutic efficacy for brain tumors has driven the continued search for novel therapies. Although the ENU–CNS tumor model has been known for over 30 years, there are relatively few reports of therapeutic trials try to inhibit the process of tumor induction or progression in rats. Particularly attractive are therapies that limit the growth or progression of the glioma by modulating the proliferative rate of either the tumor or the tumor's vasculature. Both chemopreventative and anti-angiogenic therapies have been proposed as methods for blocking tumor formation and growth. However, many of the chemopreventative agents are gaining recognition as potentially having anti-angiogenic properties. As described above, VEGF has been shown to be expressed very early in the brain tumors induced by ENU [48,49]. All-trans retinoic acid (RA), 13-cis RA and all-trans retinol reduced VEGF secretion by human keratinocytes in primary cultures [57]. Reductions were observed at concentrations as low as 10^{-10} M for all-trans RA, a level that is easily reached *in vivo* during retinoid treatment.

Increased cyclooxigenase (Cox) activity has also been reported to simulate angiogenesis [58]. The ability of NSAIDs (non-selective Cox 1 and 2 inhibitors) to exert a protective effect on the development of neural tumors [31], suggests that Cox may play a role in brain tumor development as has been shown in colon cancer. Retinoids (RA, 13-cis-RA, and retinol acetate) have been shown to markedly suppress increases in amounts of Cox-2 and the production of PGE2 stimulated by phorbol myristate acetate (PMA) in human oral epithelial cells [59]. The authors also found that retinoids suppressed the induction of Cox-2 mRNA by PMA. Nuclear run-offs revealed increased rates of Cox-2 transcription after treatment with PMA; this effect was inhibited by all-trans-RA. Transient transfection experiments showed that PMA caused nearly a 2-fold increase in Cox-2 promoter activity, an effect that was suppressed by all-trans-RA [60]. Thus both inhibition of tumor growth and vascularization are potential mechanisms of action for RP in the ENU model.

It should be pointed out that previous studies with ENU-induced brain tumors have examined tumor incidence and multiplicity with either terminal or interim sacrifices. Sacrifices provide a 'snapshot in time' of tumor status in animals, and interim sacrifices to determine tumor incidence, this dramatically increases animal group size required for statistical validity, and requires serial histological sectioning for tumor detection. The detection of time of initial tumor formation (macroscopic), the development of multiple tumors, and serial measurements of growth rates have not been previously demonstrated for individual animals. Using the MRI approach, time-to-tumor incidence appears to be an especially sensitive early endpoint marker. The lack of a significant increase in the survival time by RP in this study is perplexing, especially in light of our previous study, which did find RP to increase survival time [37]. There are several possible explanations. First, the number of animals used in this pilot study was small. This limited the statistical power to determine survival differences, which was further limited by the censoring of animals (no reported death or autopsy) at the end of the study. Second, this study used Fisher-344 rats while our previous study used Sprague-Dawley rats. Both strains are susceptible to ENU-induced tumor formation, but the results of the effectiveness of RP in increasing survival may indicate a strain difference. Finally, and potentially the most important, was the alteration in the day of transplacental tumor induction from day 15 in the previous study to day 21 in the current study.

Although our intention was to maximize the number of tumors induced by ENU, we may also have unexpectedly altered the ratios and locations of observed CNS tumor types. We discovered a large number of spinal cord tumors at terminal sacrifice: 3/12 animals in the control and 6/12 animals in the RP treated group (each group had one animal censored from analysis due to lack of autopsy), a more frequent observation than in our previous study. Others have also observed this increased frequency of spinal cord tumors resulting from chemical induction late in the gestation period or postnatally [20,61,62]. The occurrence of rapidly growing spinal cord tumors in the rat is far more lethal due to the limited space available for tumor expansion in the spine. Thus, the lack of increased survival by the RP-treated animals is a complex problem, which further illustrates the difficulty in the interpretation of survival studies with this model.

We demonstrated the ability to measure the therapeutic interventional capability in the ENU model utilizing the anti-angiogenic drug SU-5416 in a small pilot study. SU-5416 has been previously shown to reduce the growth rate of an implanted high-grade glioma cell line [41]. In our experiment, SU-5416 inhibited tumor growth in each of the three animals treated. Two animal tumors were growth arrested, while a third animal's tumor appeared to have regressed, but we are unable to exclude that this was an artifact of the MRI or a large blood vessel since we were unable to obtain serial images in time of this tumor. Although SU-5416 was able to reduce the growth rate of tumors this compound appeared to not alter the presumed progression from lower to higher grades. Treatment with SU-5614 yielded small tumors with high-grade pathology, but with a marked absence of endothelial proliferation. The detection of hemaciderin with tumors treated with SU-5614 suggests that blood had leaked out of the vasculature during treatment. The significance of this observation needs to be examined both experimentally and clinically with anti-angiogenic treatments. Unfortunately, using MRI we are unable to accurately define tumor grade at the time of therapy initiation, so potentially the tumors were undergoing progression prior to therapy. Alternatively, inhibitors of angiogenesis such as SU-5416, while affecting tumor vasculature, do not alter the biological progression of the tumor cells within the tumor.

In conclusion, we have demonstrated that MRI images can provide meaningful information on tumor incidence, multiplicity, and growth rates in a spontaneously occurring brain tumor model. They provide early non-invasive endpoints, which can easily be correlated with the survival of the animal. The ability to perform repeated measurements to detect tumor occurrence and growth of the spontaneous tumors, reduces the number of animals needed for a study. In addition, the ENU-induced brain tumor model is a well-characterized animal model with initial low-grade tumors progressing to higher grades. We have demonstrated the feasibility of utilizing this model to test for either the chemopreventative or therapeutic efficacy of drugs on these spontaneous developing tumors before their progression to a high-grade tumor phenotype.

References

1. Boring CC, Squires TS, Tong T: Cancer statistics, 1992 (Published erratum appears in CA Cancer J Clin; 42(2): 127–8, 1992). CA a Cancer J Clin 42: 19–38, 1992
2. Legler JM, Ries LA, Smith MA, Warren JL, Heineman EF, Kaplan RS, Linet MS: Cancer surveillance series (corrected): brain and other central nervous system cancers: recent trends in incidence and mortality (published erratum appears in J Natl Cancer Inst 1999 Oct 6; 91(19): 1693) (see comments). J Natl Cancer Inst 91: 1382–1390, 1999
3. Hoshino T, Rodriguez LA, Cho KG, Lee KS, Wilson CB, Edwards MS, Levin VA, Davis RL: Prognostic implications of the proliferative potential of low-grade astrocytomas. J Neurosurg 69: 839–842, 1988
4. Kepes JJ, Whittaker CK, Watson K, Morantz RA, Millett R, Clough CA, Oxley DK: Cerebellar astrocytomas in elderly patients with very long preoperative histories: Report of three cases. Neurosurgery 25: 258–264, 1989
5. Laws ER, Jr., Taylor WF, Clifton MB, Okazaki H: Neurosurgical management of low-grade astrocytoma of the cerebral hemispheres. J Neurosurg 61: 665–673, 1984
6. Piepmeier JM: Observations on the current treatment of low-grade astrocytic tumors of the cerebral hemispheres. J Neurosurg 67: 177–181, 1987
7. Piepmeier J, Christopher S, Spencer D, Byrne T, Kim J, Knisel JP, Lacy J, Tsukerman L, Makuch R: Variations in the natural history and survival of patients with supratentorial low-grade astrocytomas. Neurosurgery 38: 872–879, 1996
8. Soffietti R, Chio A, Giordana MT, Vasario E, Schiffer D: Prognostic factors in well-differentiated cerebral astrocytomas in the adult (see comments). Neurosurgery 24: 686–692, 1989
9. Medbery CAI, Straus KL, Steinberg SM, Cotelingam JD, Fisher WS, Medbery CA: Low-grade astrocytomas: Treatment results and prognostic variables. Int J Radiat Oncol Biol Phys 15: 837–841, 1988
10. Muller W, Afra D, Schroder R: Supratentorial recurrences of gliomas. Morphological studies in relation to time intervals with astrocytomas. Acta Neurochir (Wien) 37: 75–91, 1977
11. Sehgal A: Molecular changes during the genesis of human gliomas. Semin Surg Oncol 14: 3–12, 1998

12. Chung R, Whaley J, Kley N, Anderson K, Louis D, Menon A, Hettlich C, Freiman R, Hedley-Whyte ET, Martuza R, et al.: TP53 gene mutations and 17p deletions in human astrocytomas. Genes Chromosomes Cancer 3: 323–331, 1991
13. Kiebert GM, Curran D, Aaronson NK, Bolla M, Menten J, Rutten EH, Nordman E, Silvestre ME, Pierart M, Karim AB: Quality of life after radiation therapy of cerebral low-grade gliomas of the adult: results of a randomised phase III trial on dose response (EORTC trial 22844). EORTC Radiotherapy Co-operative Group. Eur J Cancer 34: 1902–1909, 1998
14. Nakamura M, Konishi N, Tsunoda S, Nakase H, Tsuzuki T, Aoki H, Sakitani H, Inui T, Sakaki T: Analysis of prognostic and survival factors related to treatment of low-grade astrocytomas in adults. Oncology 58: 108–116, 2000
15. Olson JD, Riedel E, DeAngelis LM: Long-term outcome of low-grade oligodendroglioma and mixed glioma (In Process Citation). Neurology 54: 1442–1448, 2000
16. Reddy AT, Packer RJ: Chemotherapy for low-grade gliomas. Childs Nerv Syst 15: 506–513, 1999
17. Druckrey H, Ivankovic S, Gimmy J: Cancerogenic effects of methyl- and ethyl-nitrosourea (MNU and ENU) at single intracerebral and intracarotidal injection in newborn and young BD-rats. Z Krebsforsch Klin Onkol Cancer Res Clin Oncol 79: 282–297, 1973
18. Ivankovic S, Druckrey H: Transplacental induction of malignant tumors of the nervous system. I. Ethyl-nitroso-urea (ENU) in BD IX rats. Z Krebsforsch Klin Onkol Cancer Res Clin Oncol 71: 320–360, 1968
19. Koestner A: Characterization of N-nitrosourea-induced tumors of the nervous system; their prospective value for studies of neurocarcinogenesis and brain tumor therapy. Toxicol Pathol 18: 186–192, 1990
20. Naito M, Naito Y, Ito A: Strain differences of tumorigenic effect of neonatally administered N-ethyl-N-nitrosourea in rats. Gann 73: 323–331, 1982
21. Koestner A, Swenberg JA, Wechsler W: Transplacental production with ethylnitrosourea of neoplasms of the nervous system in Sprague-Dawley rats. Am J Pathol 63: 37–56, 1971
22. Vaquero J, Coca S, Zurita M, Oya S, Arias A, Moreno M, Morales C: Synaptophysin expression in 'ependymal tumors' induced by ethyl-nitrosourea in rats. Am J Pathol 141: 1037–1041, 1992
23. Vaquero J, Oya S, Coca S, Zurita M: Experimental induction of primitive neuro-ectodermal tumours in rats: a re-appraisement of the ENU-model of neurocarcinogenesis. Acta Neurochir 131: 294–301, 1994
24. Wechsler W: Old and new concepts of oncogenesis in the nervous system of man and animals. Prog Exp Tumor Res 17: 210–278, 1972
25. Wechsler W, Rice JM, Vesselinovitch SD: Transplacental and neonatal induction of neurogenic tumors in mice: comparison with related species and with human pediatric neoplasms. National Cancer Institute Monographs 219–226, 1979
26. Zook BC, Simmens SJ, Jones RV: Evaluation of ENU-induced gliomas in rats: nomenclature, immunochemistry, and malignancy. Toxicol Pathol 28: 193–201, 2000
27. Mandeville R, Franco E, Sidrac-Ghali S, Paris-Nadon L, Rocheleau N, Mercier G, Desy M, Devaux C, Gaboury L: Evaluation of the potential promoting effect of 60 Hz magnetic fields on N-ethyl-N-nitrosourea induced neurogenic tumors in female F344 rats. Bioelectromagnetics 21: 84–93, 2000
28. Alexandrov VA, Bespalov VG, Boone CW, Kelloff GJ, Malone WF: Study of postnatal effects of chemopreventive agents on offspring of ethylnitrosourea-induced transplacental carcinogenesis in rats. I. Influence of retinol acetate, alpha-tocopherol acetate, thiamine chloride, sodium selenite, and alpha-difluoromethylornithine. Cancer Lett 60: 177–184, 1991
29. Alexandrov VA, Bespalov VG, Petrov AS, Troyan DN, Lidaks M: Study of post-natal effect of chemopreventive agents on ethylnitrosourea-induced transplacental carcinogenesis in rats. III. Inhibitory action of indomethacin, voltaren, theophylline and epsilon-aminocaproic acid. Carcinogenesis 17: 1935–1939, 1996
30. Bespalov VG, Aleksandrov VA, Petrov AS, Troian DN: The inhibiting effect of epsilon-aminocaproic acid on the incidence of induced tumors of the esophagus, nervous system and kidneys. Vopr Onkol 38: 69–74, 1992
31. Bespalov VG, Aleksandrov VA, Petrov AS, Lidak M: The inhibiting effect of ortofen and indomethacin in relation to the development of induced nervous system tumors in rats. Eksp Klin Farmakol 56: 52–54, 1993
32. Ross BD, Zhao YJ, Neal ER, Stegman LD, Ercolani M, Ben-Yoseph O, Chenevert TL: Contributions of cell kill and posttreatment tumor growth rates to the repopulation of intracerebral 9L tumors after chemotherapy: an MRI study. Proc Natl Acad Sci USA 95: 7012–7017, 1998
33. Lasker SE, latropoulos MJ, Hecht SS, Misra B, Amin S, Zang E, Williams GM: N-ethyl-N-nitrosourea induced brain tumors in rats monitored by nuclear magnetic resonance imaging, plasma proton nuclear magnetic resonance spectroscopy and microscopy. Cancer Lett 67: 125–131, 1992
34. Nakajima M, Nakasu S, Morikawa S, Inubushi T: Estimation of volume doubling time and cell loss in an experimental rat glioma model *in vivo*. Acta Neurochir 140: 607–612, 1998
35. Schmiedl UP, Kenney J, Maravilla KR: Dyke Award Paper. Kinetics of pathologic blood-brain-barrier permeability in an astrocytic glioma using contrast-enhanced MR. Ajnr: Am J Neuroradiol 13 5–14, 1992
36. Yamada K, Chen CJ, Satoh H, Hirota T, Aoyagi K, Enkawa T, Ozaki Y, Sekiguchi F, Furuhama K: Magnetic resonance imaging of rat head with a high-strength (4.7 T) magnetic field. J Veterinary Med Sci 59: 303–306, 1997
37. Ross DA, Kish P, Muraszko KM, Blaivas M, Strawderman M: Effect of dietary vitamin A or N-acetylcysteine on ethylnitrosourea-induced rat gliomas. J Neuro-Oncol 40: 29–38, 1998
38. Guerin C, Laterra J: Regulation of angiogenesis in malignant gliomas. Exs 79: 47–64, 1997
39. Jensen RL: Growth factor-mediated angiogenesis in the malignant progression of glial tumors: a review. Surg Neurol 49: 189–195; discussion 196, 1998
40. Lund EL, Spang-Thomsen M, Skovgaard-Poulsen H, Kristjansen PE: Tumor angiogenesis – a new therapeutic

target in gliomas. Acta Neurol Scand 97: 52–62, 1998
41. Menger MD, Volmar B, Schilling L, Schmiedek P, Hirth KP, Ullrich A, Fong TAT, Vajkoczy P: Inhibition of tumor growth, angiogenesis, and microcirculation by the novel Flk-1 inhibitor SU5416 as assessed by intravital multi-fluorescence videomicroscopy. Neoplasia 1: 31–41, 1999
42. Donovan PJ: Cell sensitivity to transplacental carcinogenesis by N-ethyl-N-nitrosourea is greatest in early post-implantation development. Mutat Res 427: 59–63, 1999
43. Weinzweig J, Levenson SM, Rettura G, Weinzweig N, Mendecki J, Chang TH, Seifter E: Supplemental vitamin A prevents the tumor-induced defect in wound healing. Ann Surg 211: 269–276, 1990
44. Galloway PG, Likavec MJ, Perry G: Immunohistochemical recognition of ethylnitrosourea induced rat brain microtumors by anti-Leu 7 monoclonal antibody. Cancer Lett 49: 243–248, 1990
45. Ikeda T, Mashimoto H, Iwasaki K, Shimokawa I, Matsuo T: A sequential ultrastructural and histoautoradiographic study of early neoplastic lesions in ethylnitrosourea-induced rat glioma. Acta Pathologica Japonica 39: 487–495, 1989
46. Yoshino T, Motoi M, Ogawa K: Morphological maturation of tumor cells induced by ethylnitrosourea (ENU) in rat brains. I. On the tumors by administration of ENU in the late gestational stage. Acta Pathologica Japonica 35: 1385–1396, 1985
47. Yoshino T, Motoi M, Ogawa K: Immunohistochemical studies on cellular character of microtumors induced by ethylnitrosourea in the rat brain utilizing anti-Leu 7 and anti-glial fibrillary acidic protein antibodies. Acta Neuropathologica 66: 167–169, 1985
48. Okimoto T, Shimokawa I, Higami Y, Ikeda T: VEGF and bFGF mRNA are expressed in ethylnitrosourea-induced experimental rat gliomas. Cell Mol Neurobiol 17: 141–150, 1997
49. Yoshimura F, Kaidoh T, Inokuchi T, Shigemori M: Changes in VEGF expression and in the vasculature during the growth of early-stage ethylnitrosourea-induced malignant astrocytomas in rats. Virchows Archiv 433: 457–463, 1998
50. Arbiser JL, Moses MA, Fernandez CA, Ghiso N, Cao Y, Klauber N, Frank D, Brownlee M, Flynn E, Parangi S, Byers HR, Folkman J: Oncogenic H-ras stimulates tumor angiogenesis by two distinct pathways. Proc Natl Acad Sci USA 94: 861–866, 1997
51. Folkman J, Hanahan D: Switch to the angiogenic phenotype during tumorigenesis. Princess Takamatsu Symposia 22: 339–347, 1991
52. Folkman J: The role of angiogenesis in tumor growth. Semin Cancer Biol 3: 65–71, 1992
53. Abdulrauf SI, Edvardsen K, Ho KL, Yang XY, Rock JP, Rosenblum ML: Vascular endothelial growth factor expression and vascular density as prognostic markers of survival in patients with low-grade astrocytoma. J Neurosurg 88: 513–520, 1998
54. Wrba H, Dutter A, Hacker-Rieder A: Influence of vitamin A on the formation of ethylnitrosourea (ENU)-induced leukemias. Arch Geschwulstforsch 53: 89–92, 1983
55. Wrba H, Dutter A, Hacker-Rieder A, Abdel-Galil AM: Prevention of transplacentally induced malignant diseases. Oncology 41: 33–35, 1984
56. Grubbs CJ, Hill DL, Farnell DR, Kalin JR, McDonough KC: Effect of long-term administration of retinoids on rats exposed transplacentally to ethylnitrosourea. Anticancer Res 5: 205–209, 1985
57. Weninger W, Rendl M, Mildner M, Tschachler E: Retinoids downregulate vascular endothelial growth factor/vascular permeability factor production by normal human keratinocytes. J Invest Dermatol 111: 907–911, 1998
58. Chiarugi V, Magnelli L, Gallo O: Cox-2, iNOS and p53 as play-makers of tumor angiogenesis (review). Int J Mol Med 2: 715–719, 1998
59. Mestre JR, Subbaramaiah K, Sacks PG, Schantz SP, Dannenberg AJ: Phorbol ester-mediated induction of cyclooxygenase-2 gene expression is inhibited by retinoids. Ann NY Acad Sci 833: 173–178, 1997
60. Mestre JR, Subbaramaiah K, Sacks PG, Schantz SP, Tanabe T, Inoue H, Dannenberg AJ: Retinoids suppress phorbol ester-mediated induction of cyclooxygenase-2. Cancer Res 57: 1081–1085, 1997
61. Naito M, Naito Y, Ito A: Effect of age at treatment on the incidence and location of neurogenic tumors induced in Wistar rats by a single dose of N-ethyl-N-nitrosourea. Gann 72: 569–577, 1981
62. Naito M, Naito Y, Ito A: Spinal tumors induced by neonatal administration of N-ethyl-N-nitrosourea in Wistar rats. Gann 72: 30–37, 1981

Address for offprints: Phillip E. Kish, Department of Neurosurgery, University of Michigan, 1500 East Medical Center Drive, 2128 Taubman, Box 0338, Ann Arbor, MI 48109-0338, USA; Tel.: (734) 936-5062; E-mail: pkish@umich.edu